Available online at www.sciencedirect.com

ScienceDirect

Procedia CIRP 124 (2024) 776–780

www.elsevier.com/locate/procedia

13th CIRP Conference on Photonic Technologies [LANE 2024], 15-19 September 2024, Fürth, Germany

Real-time grid detection in sheet metal fiber laser cutting through coaxial monitoring

Sofia Guerra[a,*], Leonardo Caprio[a], Matteo Pacher[c], Davide Gandolfi[c], Barbara Previtali[a], Sergio M. Savaresi[b], Mara Tanelli[b]

[a]*Department of Mechanical Engineering, Politecnico di Milano, Via La Masa 1, 20156 Milan, Italy*
[b]*Department of Electronics, Information and Bioengineering, Politecnico di Milano, Via G. Ponzio 34/5, 20133 Milano, Italy*
[c]*Adige S.p.A., BLM GROUP, Via per Barco 11, 38056 Levico Terme (TN), Italy*

* Corresponding author. Tel.: +39-3314241919; *E-mail address:* sofia.guerra@polimi.it

Abstract

Real-time defects' estimation and control of the cut quality through the coaxial camera monitoring of the kerf are amongst the most promising developments for laser cutting. In industrial systems, sheets are positioned on a metallic grid creating discontinuities in the cutting process due to unpredictable thickness, blown and resolidified material and the time varying position of the grid. The interaction between laser radiation escaping from the kerf and the grid, along with the difficult outflow of molten material, causes changes in the process emission images. These changes influence the defect estimation approach, and, consequently, the control action. In this work, a real-time grid identification and classification-based machine learning algorithm was developed and tested during the fusion cutting of 6 mm thick Al5754, exploiting a NIR coaxial monitoring system. Real-time control experiments with dross estimates were performed, demonstrating a correct identification of the grid and highlighting a feasible industrial application.

Keywords: Laser cutting; grid identification; coaxial monitoring; machine learning;

1. Introduction

In-situ monitoring of the laser material interaction is a fundamental aspect to derive information in real-time regarding the state of the laser cutting process [1,2]. Various works in literature have studied and proved a strong correlation between the formation of defects and process emission, for both fusion [3] and flame [4] laser cutting. Through the years, coaxial camera monitoring has been proposed as a promising solution to detect the cutting process conditions [5] and build quality defects' estimation (*Duflou et al.* [6,7]). *Pacher et al.* [8,9,10] developed a real-time dross estimation via Convolutional Neural Network (CNN) based on the extraction of geometrical features of the melt pool from process emission images. Furthermore, the authors implemented a real-time speed control algorithm capable of improving cut quality and boosting productivity in fusion laser cutting. On the other hand, such approaches have been implemented only in limited scientific scenarios regarding specific cases but never tested in real-life industrial applications.

In industrial systems, metal sheets are positioned on a metallic grid that sustains the plate during the entire cutting operation. It is not possible to define a priori a laser grid map due to its interchangeable position accordingly to different applications. Moreover, during the cutting process blown and resolidified wasted material adheres to the laser grid, resulting in unpredictable thickness. The effects of laser grid on camera sensor images have not been thoroughly explored in literature; academic articles primarily concentrate on analyzing the constraints of the supporting grid solely to enhance the nesting

10.1016/j.procir.2024.08.223

phase (*Struckmeier et al.* [11,12]). However, the interaction between laser radiation escaping from the kerf and the grid, along with the difficult outflow of molten material, causes changes in the captured images, which are characterized by a significant increase of the intensity and geometrical dimensions of the melt pool. These changes on the recorded images strongly affect the geometrical feature extraction upon which the Machine Learning (ML) models of the defects' prediction are based. For these reasons, although the grid represents an essential supportive element to the metal plate in industrial applications, its presence strongly hinders the reliability of the defects' estimation approach thus influencing the feedback control performances.

Within this framework, the development of a robust classification algorithm capable of detecting the presence of the grid and adjusting or disabling the control action accordingly plays a crucial role for the industrial applicability of feedback control approaches. The current work proposes a real-time grid identification and classification-based machine learning algorithm that has been developed and tested during the fusion cutting of 6 mm thick Al5754, exploiting a NIR coaxial monitoring system. A novel control architecture with laser grid supervisor has been implemented. Furthermore, real-time speed control experiments with dross estimates were performed, demonstrating a correct identification of the laser grid that paves the way for a feasible industrial application of this approach.

2. Materials and Methods

2.1. Materials

The experiments of this research work were carried out on aluminium Al5754 with thickness 6 mm. The nominal chemical composition is reported in Table 1.

Table 1. Chemical composition of aluminum Al5754 (wt%).

Si	Mn	Cu	Mg	Zn	Cr	Ti	Mn+Cr	Al
0.40	0.50	0.10	3.6	0.20	0.30	0.15	0.6	balanced

2.2. Laser cutting and monitoring system

The experiments in this research utilized an industrial laser cutting machine (*LC5, BLM Group, Levico Terme, Italy*). The system is equipped with a laser cutting head featuring a collimating lens with focal length of 100 mm and a focusing lens with focal length of 200 mm (*HPSSL, Precitec, Gaggenau, Germany*). A 6 kW laser source emitting at λ=1070 nm from a transport fiber diameter of 100 µm was employed (*YLS-6000-CUT, IPG Photonics, Cerro Maggiore, Italy*).

The cutting head is equipped with a coaxial monitoring system, enabling observation of the process emission. The monitoring architecture, previously detailed in past publications [8,9,10], consists of a CMOS industrial camera (*XiQ MQ013MG-ON, Ximea, Munster, Germany*) utilising Si photodetectors and near infrared wavelength filtration to capture the process dynamics. The band pass and short pass filter are centered at 750 nm and 1000 nm, respectively. The imaging chain observes the laser-material interaction with a spatial resolution of 9.6 µm/pixel. Process emissions images were acquired at 750 Hz with an exposure time of 400 µs. A STM32 microcontroller (*NUCLEOF767ZI, STMicroelectronics, Geneva, Switzerland*) was employed to realize real-time control experiments with a control frequency of 375 Hz. The overall configuration of the laser cutting and monitoring system is reported in Table 2.

Table 2. Laser cutting and monitoring system specifications.

Laser system specifications	Values
Maximum emission power, P_{max} [W]	6000
Emission wavelength, λ [nm]	1070
Beam quality factor, M^2	11.7
Collimation lens, f_{col} [mm]	100
Focal lens, f_{foc} [mm]	200
Fiber core diameter, d_{core} [µm]	100
Beam waist diameter, d_{waist} [µm]	200
Monitoring system	**Values**
Acquisition frequency, $f_{acq,}$ [Hz]	750
Control frequency, f_{ctrl} [Hz]	375
Spatial resolution, SR [µm/pixel]	9.6
Camera exposure time, $t_{exp,}$ [µs]	400
Observation wavelength, λ_{obs} [nm]	750±10
Field of View, FOV [pixel x pixel]	320 x 320

2.3. Experimental design and Machine Learning approach

An experimental study was designed exploiting a supervised machine learning approach to develop a real-time classification algorithm to the detect the presence of the supporting grid structure while cutting a 6 mm thick Al sheet (as shown in the experimental set up of Fig. 1a). Linear cuts were performed transversally with respect to the supporting grid at different levels of cutting velocity whilst the monitoring chain allowed to observe and capture process emission images (Fig. 1b). The acquired frames were then labelled according to the presence of the supporting grid and were used as training and testing dataset for the real-time grid identification algorithm.

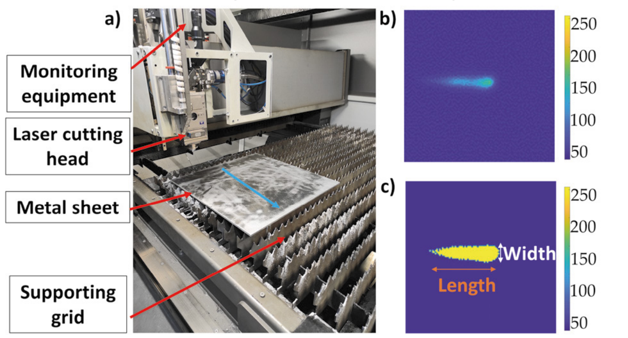

Fig. 1. (a) Laser cutting system with the grid sustaining the metal sheet and cut path (in blue); (b) Process emission image; (c) Geometrical feature extraction on the binarized image with a hard-threshold of 15.

Fixed parameters were chosen based on prior experiments whilst the variable factor corresponded to the cutting velocity (which is also the variable of the controller architecture employed). The laser emission power was fixed at 6kW, while employing nitrogen as an assist gas at 12.5 bar. The focal position was fixed at -5.5 mm with respect to the nozzle whilst a stand-off distance from the sheet was kept at 0.7 mm. Linear cuts according to the linear trajectory shown in Fig. 1a) were conducted at three levels of velocity (namely 2800, 3200 and 3600 mm/min) corresponding to high, middle and low dross formation conditions. Two repetitions of each experimental condition were performed. The fixed and variable parameters of the experimental design are reported in Table 3.

Table 3. Experimental design to train the supervised ML algorithm for real-time grid identification.

Fixed parameters	Values
Laser power, *P* [W]	6000
Assistant gas	N_2
Gas pressure, *p* [bar]	12.5
Focal position, *FP* [mm]	-5.5
Stand-off Distance, *SOD* [mm]	0.7
Cut length, [mm]	400
Variable parameters	
Cutting speed, *v* [mm/min]	2800; 3200; 3600

The images were binarized through hard thresholding of the grayscale images at a predetermined value of 15 (as shown in Fig 1c). The process emission images were then analyzed to extract geometrical features of the melt pool in order to obtain real-time estimation of the dross formation (as shown in prior research [8,9,10]). For each feature, both the mean and standard deviation were computed on a lookback window of 75 frames, aimed at enhancing the dimensionality of the feature space. The same features could be exploited to train classification algorithms for the real-time grid detection.

The acquired images were also labeled in accordance to the presence of the grid which could be determined given that the path, sampling frequency and position of the metal sheet were imposed. Hence, the dataset was manually labeled resulting in a set of binary numbers, *i.e.* 1 or 0, indicating the presence or absence of the grid. This information was then associated to the geometrical features of the single images.

Exploiting the dataset generated via the experimental design, different Machine Learning (ML) models were trained and tested with the aim of classifying the passage of the nozzle on the laser grid. To determine the most effective model, evaluations were conducted based on their validation and testing accuracy, as well as statistical indicators, including *Precision (P)*, *Recall (R)* and *F1 Score*. The tested ML algorithms consisted in *Linear Discriminant* (*LD*), *Linear Support Vector Machine* (*SVM*) and an *Artificial Neural Network (ANN*). The *ANN* employed is a Feed Forward network with one connected layer (of size 10) and *ReLU* (*Rectified Linear Units*) activation function, used to add non linear transformations to the output of the connected layer. The *Linear SVM* model is based on two Support Vectors and a linear Kernel. Moreover, the authors chose a ten times higher misclassification cost for the false negative (FN) grid classification conditions, with the goal of reducing the FNs rate and improving the robustness of the developed approach [13].

After training and testing the grid classification, another experimental plan was designed to validate it while performing linear cuts with an active feedback control on the cutting velocity. The developed novel control scheme is constituted by a speed regulating loop coupled with a supervisor loop dedicated to the grid identification algorithm. Fig. 2 illustrates the control architecture: *G(s)* represents the model of the laser cutting process, g_{est} represents the identification of the laser grid, v_{PI} represents the cutting speed calculated by the PI controller *PI(s)* and v_g the actual speed value when a laser grid condition is detected. Moreover, d_{est} and d_{ref} represents respectively the estimated value of dross and the setpoint level of dross which is imposed by the user to achieve a target cut quality. The regulator is a general Proportional-Integral (PI) controller where the control variable *v* in the time-domain is in the form shown in the following equation:

$$v(t) = K_p \cdot e(t) + K_i \cdot \int e(t)dt \tag{1}$$

where *e* represents the error between the reference target quality d_{ref} and the estimated variable d_{est}. The proportional part K_p and the integral part K_i were set -400 and -2750 respectively. The aim of the controller was to update the cutting speed in real-time based on the error value *e*. The PI controller modifies the cutting speed v_{PI} aiming to achieve the desired level of dross as long as the grid is not detected ($g_{est} = 0$). When the laser grid is identified by the supervisor loop ($g_{est} = 1$), the speed regulating loop of the controller maintains a fixed cutting velocity v_g until the grid is no longer detected ($g_{est} = 0$).

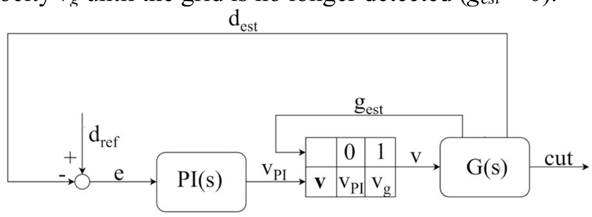

Fig. 2. Control scheme in the Laplace domain of the novel controller architecture with laser grid supervisor.

The laser grid identification algorithm was tested in real-time while performing linear cuts. Two experiments were performed to validate the novel control architecture. Each experiment aimed at a different reference quality level (i.e. the value of dross d_{ref}) while starting at different cut velocities. Hence, a high reference dross level corresponding to 0.025 mm was targeted starting from a cut velocity of 2400 mm/min, while the second run aimed achieve 0.01 mm of dross starting from a cut velocity of 4000 mm/min respectively. Table 4 outlines the fixed and variable parameters used to test the novel control architecture with the real-time laser grid identification.

Table 4. Fixed and variable parameters used to test the novel control architecture with the laser grid supervisor.

Fixed parameters	Values
PI proportional part, K_p	-400
PI integral part, K_i	-2750
Variable factors	Values
Starting sets	
Cutting speed, *v* [mm/min] – Dross reference value d_{ref} [mm]	2400 – 0.025, 4000 – 0.01

3. Results

3.1. Laser grid effects on captured images and defects estimate

The grid identification is crucial because the growth in brightness and dimension of the kerf when the nozzle passes on the grid leads to important changes in the acquired images. The intensity and geometrical dimensions of the melt pool significantly increase, as evidenced by Fig. 3a and Fig. 3b, which illustrate the difference between the captured frame outside or along the grid respectively. Consequently, the extracted features from the images are subject to variations influencing the dross estimate, as shown in Fig. 3c. As it can be noticed, there is an overestimation of dross (represented in orange) with high peaks when the grid is encountered (represented in blue).

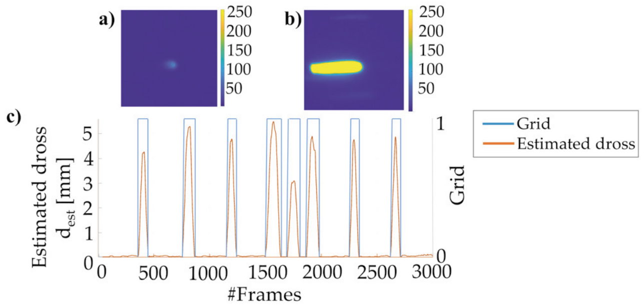

Fig. 3. Process emission images showing (a) cut without the presence of the grid and (b) with the presence of the grid; (c) Effect of the laser grid on the dross estimate.

3.2. Machine learning model selection

In this section, the performances of the trained ML models are presented and discussed. The *Linear Discriminant* exhibits the highest *Recall* value, as shown in Fig. 4. However, it is important to note that its *Precision* value is the lowest one, indicating an overestimation of false positives. Consequently, it was excluded from the final model choice. Moving forward, both the *NN* and the *Linear SVM* demonstrate excellent and comparable performances. Nonetheless, the authors opted to discard the *NN* due to its computational requirements for real-time implementation in an industrial setting into the machine architecture. Instead, the *Linear SVM* was selected as final choice, because it offers optimal overall performances with a lower computational effort.

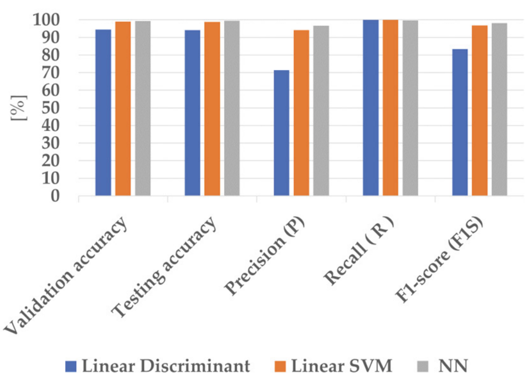

Fig. 4. Performances of the different ML models for laser grid classification.

3.3. Novel controller architecture results

In this section, the results of the real-time control experiments with the grid classification algorithm are presented. In the first scenario, when the starting speed is lower than the nominal value of 3000 mm/min, the expected behaviour is an increase of the cutting speed up to the steady-state value. Fig. 5 shows the cutting speed signal (in red) compared to the grid detection (in blue). As depicted, the cutting speed remains constant as long as a grid condition is detected and eventually reaches the steady state value, ensuring a good cut quality. Moreover, Fig. 6 shows the control experiment conducted with a starting cutting speed of 4000 mm/min. The PI controller is responsible for the reducing of the speed to the nominal value of 3000 mm/min. Similarly, when the grid condition is detected, the cutting speed provided by the PI controller remains constant, despite the dross overestimation.

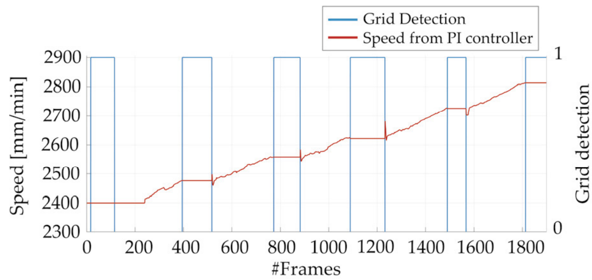

Fig. 5. Cutting speed signal compared to grid detection for a controlled cut starting from 2400 mm/min.

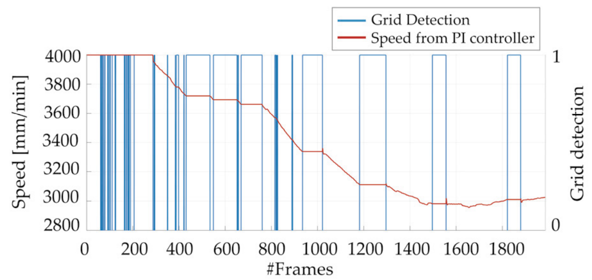

Fig. 6. Cutting speed signal compared to grid detection for a controlled cut starting from 4000 mm/min.

4. Discussion

This work studies the extension of cutting speed feedback control scheme to industrial scenarios where the laser grid has an essential supporting role, but simultaneously hinders the reliability of the control algorithm. The presented approach is based on the deactivation of the control action on the cutting speed as long as a grid condition is detected by the supervisor loop. Accordingly, considering an average 3 mm thick grid and a 2400÷4000 mm/min speed range, each grid identification introduces a delay within the range of 45÷75 ms in controlling the cutting speed signal. As future developments, robust and adaptive feedback control schemes (such as *H-infinity loop-shaping* or *Loop Transfer Recovery*) could be considered as interesting alternatives [14]. The mentioned control algorithms design different control laws addressing specific system behavior modes and could be employed for an ad hoc adjustment of the control action despite the presence of the grid. Finally, additional sensors, such as photodiodes, could be exploited to identify the grid together with the geometrical feature extraction approach, to enhance the reliability of the classification algorithm.

5. Conclusions

In this study, a real-time grid identification and classification based machine learning algorithm was developed during the fusion cutting of 6 mm thick Al5754, exploiting a NIR coaxial monitoring system to capture process emission images. Different ML algorithms were trained, and a *Linear SVM* was selected to classify the grid condition. Moreover, a novel controller architecture with laser grid supervisor was implemented and tested during real-time control experiments with dross estimation. These experiments demonstrated an effective identification of the grid and highlighted the feasibility of the proposed approach for industrial control applications.

Acknowledgements

The authors would like to thank the Italian Ministry for University and Research (MUR) for supporting the research via the National Plan for Recovery and Resilience (PNRR). Special thanks to Dario Cocci for the support throughout the experiments and research activities.

References

[1] Schleier M, Adelmann B, Neumeier B, Hellmann R. Burr formation detector for fiber laser cutting based on a photodiode sensor system. Opt Laser Technol. 2017 Nov 1;96:13–7.
[2] Levichev N, Rodrigues GC, Duflou JR. Real-time monitoring of fiber laser cutting of thick plates by means of photodiodes. In: Procedia CIRP. Elsevier B.V.; 2020. p. 499–504.
[3] Levichev N, Duflou JR. On multi-sensor monitoring of fiber laser fusion cutting. IOP Conf Ser Mater Sci Eng. 2021 Nov 1;1135(1):012014.
[4] Levichev N, Tomás García A, Duflou JR. Monitoring Opportunities in Fiber Laser Flame Cutting. Lasers in Manufacturing and Materials Processing. 2021 Dec 1;8(4):491–510.
[5] Levichev N, Costa Rodrigues G, Vorkov V, Duflou JR. Coaxial camera-based monitoring of fiber laser cutting of thick plates. Opt Laser Technol. 2021 Apr 1;136.
[6] Fallahi Sichani E, Kohl S, Duflou JR. Plasma detection and control requirements for CO2 laser cutting. CIRP Ann Manuf Technol. 2013;62(1):215–8.
[7] Duflou JR, Fallahi Sichani E, De Keuster J, Kruth JP. Development of a real time monitoring and adaptive control system for laser flame cutting. In: ICALEO, 28th International Congress on Applications of Lasers and Electro-Optics, Congress Procedings. 2009.
[8] Pacher M, Franceschetti L, Strada SC, Tanelli M, Savaresi SM, Previtali B. Real-time continuous estimation of dross attachment in the laser cutting process based on process emission images. J Laser Appl. 2020 Nov;32(4):042016.
[9] Pacher M, Strada S, Tanelli M, Previtali B, Savaresi SM, Spa A. Real-time velocity regulation for productivity optimization in laser cutting.
[10] Pacher M, Caprio L, Delama G, Gandolfi D, Savaresi SM, Previtali B, et al. Real-time roughness estimation in laser oxidation cutting via coaxial process vision. In: Lasers in Manufacturing Conference . 2023. p. 1–9.
[11] Struckmeier F, León FP. Nesting in the sheet metal industry: Dealing with constraints of flatbed laser-cutting machines. In: Procedia Manufacturing. Elsevier B.V.; 2019. p. 575–82.
[12] Struckmeier F, Zhao J, León FP. Measuring the supporting slats of laser cutting machines using laser triangulation. International Journal of Advanced Manufacturing Technology. 2020 Jun 1;108(11–12):3819–33.
[13] Jiang H. Machine Learning Fundamentals. Cambridge University Press; 2021.
[14] Nabil Derbel, Ahmed Said Nouri, Quanmin Zhu. Advances in Robust Control and Applications. Derbel N, Nouri AS, Zhu Q, editors. Vol. 474. Singapore: Springer Nature Singapore; 2023.